

Received:  
11 September 2017

Revised:  
10 January 2018

Accepted:  
15 January 2018

<https://doi.org/10.1259/bjr.20170690>

Cite this article as:

Wang KY, Chetta J, Bains P, Balzer A, Lincoln J, Uribe T, et al. Spectrum of MRI brain lesion patterns in neuromyelitis optica spectrum disorder: a pictorial review. *Br J Radiol* 2018; **91**: 20170690.

## PICTORIAL REVIEW

# Spectrum of MRI brain lesion patterns in neuromyelitis optica spectrum disorder: a pictorial review

<sup>1</sup>KEVIN YUQI WANG, MD, <sup>1</sup>JUSTIN CHETTA, MD, <sup>2</sup>PAVIT BAINS, MD, <sup>1</sup>ANTHONY BALZER, MD, <sup>3</sup>JOHN LINCOLN, MD, PhD, <sup>1</sup>TOMAS URIBE, MD and <sup>1</sup>CHRISTIE M LINCOLN, MD

<sup>1</sup>Department of Radiology, Baylor College of Medicine, Houston, TX, USA

<sup>2</sup>Radiology Associates of North Texas, Fort Worth, TX, USA

<sup>3</sup>Department of Neurology, The University of Texas Health Science Center at Houston, Houston, TX, USA

Address correspondence to: Dr Kevin Yuqi Wang  
E-mail: [yuqiw@bcm.edu](mailto:yuqiw@bcm.edu)

### ABSTRACT

Neuromyelitis optica is a neurotropic autoimmune inflammatory disease of the central nervous system traditionally thought to exclusively involve the optic nerves and spinal cord. With the discovery of the disease-specific aquaporin-4 antibody and the increasing recognition of clinical and characteristic imaging patterns of brain involvement in what is now termed neuromyelitis optica spectrum disorder (NMOSD), MRI now plays a greater role in diagnosis of NMOSD based on the 2015 consensus criteria and in distinguishing it from other inflammatory disorders, particularly multiple sclerosis (MS). Several brain lesion patterns are highly suggestive of NMOSD, whereas others may serve as red flags. Specifically, long corticospinal lesions, hemispheric cerebral white matter lesions and periependymal lesions in the diencephalon, dorsal brainstem and white matter adjacent to lateral ventricles are typical of NMOSD. In contrast, juxtacortical, cortical, or lesions perpendicularly oriented to the surface of the lateral ventricle suggests MS as the diagnosis. Ultimately, a strong recognition of the spectrum of MRI brain findings in NMOSD is essential for accurate diagnosis, and particularly in differentiating from MS. This pictorial review highlights the spectrum of characteristic brain lesion patterns that may be seen in NMOSD and further delineates findings that may help distinguish it from MS.

### INTRODUCTION

Neuromyelitis optica (NMO) is an autoimmune inflammatory disease of the central nervous system (CNS) traditionally characterized as an entity exclusively manifesting as relapsing attacks of optic neuritis and longitudinally extensive transverse myelitis (LETM). The presence of a longitudinally extensive cord lesion (spanning three or more contiguous vertebral segments) is one of the most distinct features of NMO. Involvement limited to the optic nerves and spinal cord with sparing of brain was also traditionally thought to be characteristic. However, the past decade has witnessed a dramatic increase in understanding, prompted by the discovery of the highly disease-specific aquaporin-4 (AQP4) antibody (AQP4-Ab). Diagnostic criteria prior to 2006 excluded diagnosis in patients with asymptomatic MRI brain lesions who would otherwise exhibit a typical disease course for NMO.<sup>1</sup> However, non-specific brain lesions occur in 60% of patients later in the disease course in those originally diagnosed with NMO.<sup>2</sup>

Ultimately, with incorporation of the disease-specific AQP4-Ab, the 2006 revised diagnostic criteria relaxed requirements and permitted asymptomatic brain lesions.<sup>3</sup> Moreover, the AQP4-Ab further facilitated observations that helped broaden the clinical and neuroimaging phenotype of NMO, which ultimately led to the term NMO spectrum disorders (NMOSD) in 2007. Based on these observations, NMOSD further included those with AQP4-Ab seropositivity with limited or inaugural forms of NMO (*e.g.* recurrent optic neuritis without LETM), AQP4-Ab seropositivity in those with systemic lupus erythematosus and Sjogren syndrome, as well as those diagnosed as Asian opticospinal multiple sclerosis.<sup>1</sup> A further revision in 2015 unified the previous NMO definition of 2006 and NMOSD definition of 2007. With the recognition of the high incidence of brain involvement, diagnosis in seropositive patients may now occur in almost any CNS region involvement, and for the first time, it may occur without involvement of either the optic nerves or spinal cord.<sup>4</sup> Moreover, the consensus definition devised separate criteria based on AQP4-Ab

serological status, given the higher degree of diagnostic uncertainty and heterogeneity in seronegative patients and the need for more stringent seronegative criteria.<sup>4</sup>

Overall, with the increasingly broadening phenotype and recognition of brain involvement as one of the hallmarks of NMOSD, it is clear that MRI plays an increasingly central role in helping differentiate NMOSD from other inflammatory disorders, particularly . Distinguishing MS and NMOSD is essential as the latter often portends a poorer prognosis and entails distinct treatments.<sup>3</sup> In fact, recent evidence suggests that some therapies utilized in treating MS may worsen NMOSD.<sup>3,5</sup> Additionally, differentiation is important in avoiding enrollment of NMOSD patients in MS trials. MRI also plays a greater role in diagnosing seronegative NMOSD patients as criteria are more stringent in this group and seronegative patients often have mixed and overlapping clinical and imaging features of NMOSD and MS. Diagnosis is further complicated by recent observations that some patients with serum myelin-oligodendrocyte glycoprotein antibody but not AQP4-Ab also demonstrate clinical and imaging features of NMOSD, suggesting a different pathogenesis.<sup>4</sup> Such patients with serum myelin-oligodendrocyte glycoprotein antibody have been reported to have fewer relapses, more caudal myelitis, are younger and less frequently female.<sup>4,6</sup>

Ultimately, a strong recognition of the spectrum of MRI brain findings in NMOSD is critical in accurate diagnosis. Several brain lesion patterns are highly suggestive of NMOSD, whereas others may serve as red flags.<sup>4</sup> Lesions involving the diencephalon, periependymal tissues of the lateral or 4th ventricle, corpus callosum, or corticospinal tract (CST) are necessary to support the diagnosis of NMOSD. In this pictorial review, we present the spectrum of typical NMOSD brain lesions in NMOSD from a single institutional series of subjects diagnosed based on 2015 consensus criteria.

## SUMMARY

### Clinical and demographic characteristics

28 NMOSD cases diagnosed based on 2015 consensus criteria were reviewed. The mean age was 41.9 years old (range of 27–74 years old). The mean age at the time of diagnosis was 34.4 years old (range of 6–68 years old). 23 (83%) were female gender. 20 (71%) were seropositive for AQP4-Ab. Of 26 patients, 14 (54%) initially presented with ON, 6 (23%) initially presented with transverse myelitis and 6 (23%) initially presented with symptoms near-simultaneously related to both. Two were diagnosed at an outside institution and initial presentations were unavailable.

### Imaging characteristics

The 2015 consensus criteria recognize the relatively high incidence of brain MRI abnormalities in NMOSD patients, with the incidence ranging from 50 to 85% based on the 2006 revised diagnostic criteria, and 51 to 89% in seropositive patients with NMOSD.<sup>6</sup> In our series, 24 (86%) cases demonstrated brain MRI abnormalities. Variation in frequency between existing studies has been hypothesized to be partly due to brain lesions becoming more prevalent with disease duration. A summary of the typical brain lesion patterns in NMOSD as reported by Wingerchuk

Table 1. Typical NMOSD Brain Lesion Patterns on MRI

1. Diencephalon lesions involving the thalamus and hypothalamus adjacent to third ventricle
2. Cerebellar and dorsal brainstem lesions adjacent to fourth ventricle
3. Dorsal medulla lesions, particularly the area postrema
4. Long, contiguous CST lesions
5. Hemispheric deep or subcortical cerebral white matter lesions
6. Periventricular white matter lesions adjacent to lateral ventricle, including corpus callosum

CST, corticospinal tract; NMOSD, neuromyelitis optica spectrum disorder.

et al<sup>4</sup> is provided in Table 1, and the prevalence of these brain lesions in our series is provided in Table 2.

### Non-specific supratentorial white matter lesions

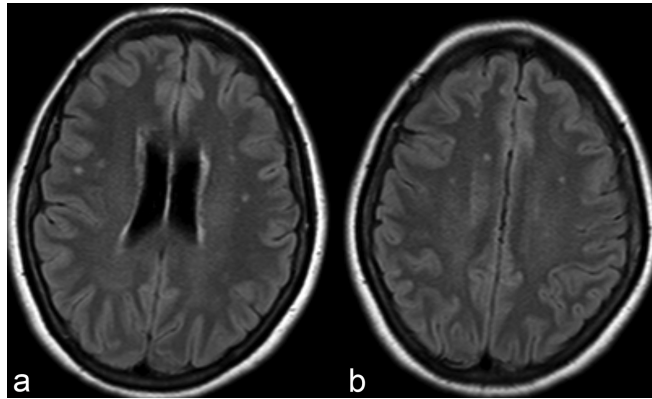
Non-specific subcortical or deep white matter small foci of hyperintensity on  $T_2$  weighted sequences are the most common brain imaging finding observed in NMOSD patients<sup>6</sup> (Figure 1). These lesions are commonly asymptomatic. Prior studies have reported incidence ranging from 35 to 84%, with longitudinal studies demonstrating asymptomatic white matter lesions accumulating in 60% of NMOSD patients.<sup>6</sup> Up to 16% of such lesions fulfil Barkhof criteria for MS,<sup>6</sup> and while such findings do not exclude NMOSD as a diagnosis, additional characteristic

Table 2. Summary of the Spectrum of Brain Lesions in 28 Patients with NMOSD based on 2015 Consensus Diagnostic Criteria

Imaging finding	Frequency
Periependymal lesions	
Diencephalon	5/28
Dorsal brainstem/cerebellum	13/28
Lateral periventricular	15/28
Absent	7/28
Enhancement	
Cloud-like	2/28
Nodular	1/28
Pencil-thin	2/28
Ring	1/28
Leptomeningeal	1/28
Absent	23/28
Diffusivity	
Increased	9/28
No change	19/28
Other	
CST lesions	2/28
Cerebral hemispheric lesions	4/28

CST, corticospinal tract; NMOSD, neuromyelitis optica spectrum disorder.

Figure 1. Axial FLAIR at the level of coronal radiata (a) and centrum semiovale (b) demonstrate punctate hyperintensities within the bilateral frontoparietal subcortical and deep white matter. While the most common imaging finding in NMOSD patients, such findings are completely non-specific and non-contributory in aiding in diagnosis. FLAIR, fluid attenuation inversion recovery; NMOSD, neuromyelitis optica spectrum disorder.



imaging findings as alluded to below are needed to confidently differentiate NMOSD from MS (Table 3).

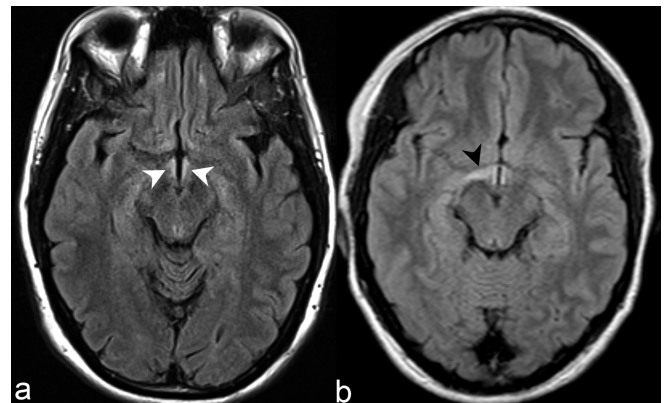
*Diencephalic lesions surrounding third ventricle and cerebral aqueduct*

Diencephalic lesions involve the periependymal surfaces of the midbrain adjacent to the cerebral aqueduct and thalamus or hypothalamus adjacent to the third ventricle (Figure 2). Accordingly, lesions within these regions correspond to areas of high AQP-4 expression.<sup>7</sup> Diencephalic periependymal involvement was seen in 5 of 28 cases (17%) in our series. Such involvement is considered atypical and exceptional for MS and relatively characteristic but not pathognomonic for NMOSD.<sup>4</sup> Moreover, symptomatic narcolepsy or acute diencephalic syndrome with typical diencephalic lesions on imaging is considered one of the core clinical characteristics in the 2015 revised diagnostic criteria.<sup>4</sup>

*Dorsal brainstem lesions surrounding fourth ventricle*

Periependymal dorsal brainstem and cerebellar lesions adjacent to the fourth ventricle, particularly in the region of the

Figure 2. (a) Axial FLAIR demonstrates abnormally increased signal intensity in the bilateral hypothalamic periependymal tissues adjacent to third ventricle (white arrow heads). (b) Axial FLAIR in a different patient demonstrates more extensive involvement of right hypothalamus (black arrow head) in comparison to the left. Such hypothalamic periependymal involvement is considered atypical and exceptional for MS and relatively characteristic but not pathognomonic NMOSD. FLAIR, fluid attenuation inversion recovery; NMOSD, neuromyelitis optica spectrum disorder; MS, multiple sclerosis.



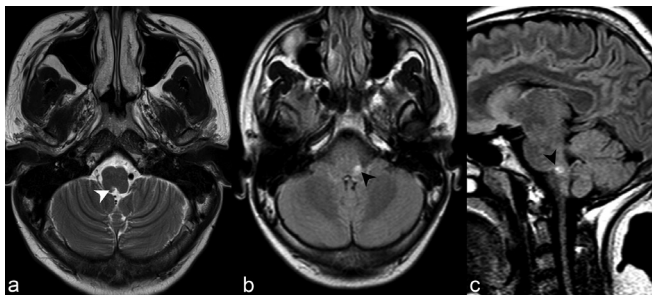
area postrema within the dorsal medulla (Figure 3), are the most specific imaging findings in the brain for NMOSD and correspond to areas of high AQP-4 expression.<sup>6,7</sup> Not surprisingly, dorsal medulla lesions are highly associated with area postrema syndrome, clinically entailing hiccups, nausea and vomiting,<sup>6</sup> and is one of the core clinical characteristics in the 2015 revised diagnostic criteria.<sup>4</sup> Lesions in the medulla are often small, linear, bilateral in distribution, and can be contiguous with lesions in the upper cervical cord.<sup>4</sup> Moreover, extension of a cervical lesion into the brainstem is considered characteristic for NMOSD.<sup>4</sup> Periependymal dorsal midbrain, pontine (Figure 4) and cerebellar lesions (Figure 5) are also considered typical for NMOSD. In the context of a seronegative patient with an acute brainstem syndrome (another core clinical characteristic in the 2015 revised diagnostic criteria), corresponding periependymal brainstem lesions on imaging

Table 3. Distinguishing Brain Lesions on MRI between NMOSD and MS

Neuromyelitis optica spectrum disorder (NMOSD)	Multiple sclerosis (MS)
Lesion intimately adjacent to lateral ventricle extending along the length of corpus callosum	Lesions oriented perpendicular to lateral ventricle (Dawson’s fingers)
Large, oedematous, heterogeneous “marbled” callosal lesions	Lesions located at inferior callosal margin or callosal-septal surface
Large, confluent hemispheric lesions	Discrete, ovoid lesions
Lesions adjacent to lateral, third and fourth ventricles along the ependymal lining	Lesions adjacent to lateral ventricle in inferior temporal lobe
Long, contiguous CST lesions	Juxtacortical U-fibre lesions
Cortical lesions rare	Cortical lesions
Perivenous lesions less common	Perivenous lesions common
Clinically silent lesions less likely	Clinically silent lesions more likely

CST, corticospinal tract; MS, multiple sclerosis; NMOSD, neuromyelitis optica spectrum disorder.

Figure 3. (a) Axial  $T_2$  weighted imaging at the level of the medulla demonstrates abnormally increased signal in the right dorsomedial medulla adjacent to the fourth ventricle in the region of the area postrema (white arrow head). The lesion was poorly visualized on FLAIR, partly secondary to the decreased sensitivity of posterior fossa lesions on such sequence. Axial (b) and sagittal (c) FLAIR of a different patient with hiccups related to area postrema syndrome demonstrate abnormally increased signal in the left dorsal medulla (black arrow heads). These lesions are often most specific for NMOSD and lesions correspond to areas of high aquaporin-4 (AQP4) expression. AQP4, high aquaporin-4; FLAIR, fluid attenuation inversion recovery; NMOSD, neuromyelitis optica spectrum disorder.



are required to satisfy criteria.<sup>4</sup> Overall, these lesions have been reported in 7 to 46% of patients with NMOSD,<sup>6</sup> and seen in 13 of 28 cases (46%) in our series.

#### Corticospinal tract lesions

CST involvement is not uncommon and found in 22 to 44% of patients.<sup>6</sup> Interestingly, only 2 cases (7%) demonstrated CST involvement in our series. Involvement may be unilateral or bilateral, and a longitudinally extensive and contiguous configuration is typical for NMOSD. For example, lesions may extend from the cerebral white matter through the posterior limb of the internal capsule and cerebral peduncles to the pons (Figure 6).<sup>8</sup> Such longitudinal configuration is analogous to LETM seen in the spine.

Figure 4. Axial 3D and 2D FLAIR at the level of the superior cerebellar peduncles (a, b) and sagittal FLAIR (c) of three different patients demonstrate foci of increased signal in the dorsal pons regional to the fourth ventricle (black arrow heads). Note the additional involvement of the CST more anteriorly with the dispersed, linear pyramidal tract bundles discretely outlined by abnormally increased signal (white arrow heads) (discussed later). 2D, two-dimensional; 3D, three-dimensional; CST, corticospinal tract; FLAIR, fluid attenuation inversion recovery.

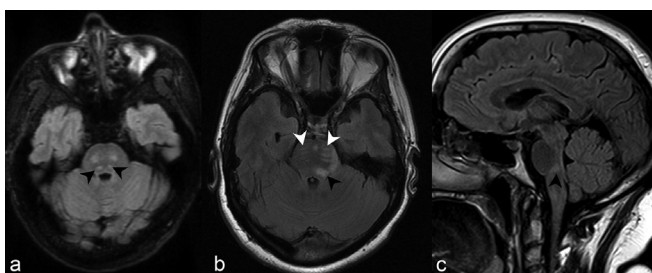
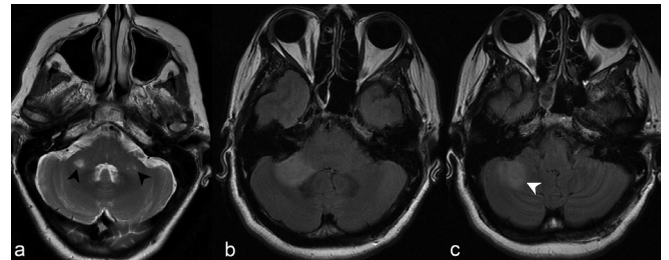


Figure 5. (a) Axial  $T_2$  weighted imaging at the level of the cerebellopontine angle demonstrates discrete foci of abnormally increased signal in both middle cerebellar peduncles (black arrow heads). (b) Axial FLAIR at the same level in another patient demonstrates a confluent focus of abnormally increased signal in the right middle cerebellar peduncle. (c) At a slightly more caudal level, the abnormal signal extends posterolaterally to involve the right cerebellar hemisphere (white arrow head). FLAIR, fluid attenuation inversion recovery.



The pathogenesis in which low AQP4-expressing CST becomes frequently involved in NMOSD remains to be determined.

#### Hemispheric cerebral white matter lesions

Hemispheric cerebral white matter lesions may suggest the diagnosis of NMOSD, but are difficult to distinguish from atypical Figure 6. Axial FLAIR images demonstrate a contiguous region of abnormally increased signal affecting the left CST (white arrowheads), from the posterior limb of the left internal capsule (a), to the cerebral peduncle (b-d) and pontine pyramidal tract bundles (e). Note the additional full-thickness involvement of the splenium of the corpus callosum, which is often termed “arch bridge pattern” (a, black arrows) (discussed later), and confluent involvement of the genu beginning to extend into the cerebral white matter (a, black arrow head). Coronal FLAIR imaging of the same patient at the level of the third ventricle (f) depicts the contiguous involvement of the left CST extending from the posterior limb of the internal capsule caudally to the cerebral peduncle (white arrow). Note again the extension of the signal abnormality from the corpus callosum into the left cerebral white matter (f, black arrow head). CST, corticospinal tract; FLAIR, fluid attenuation inversion recovery.

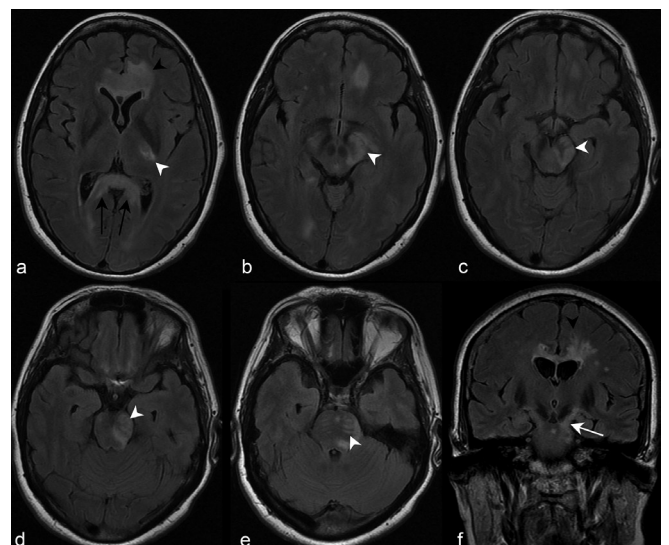
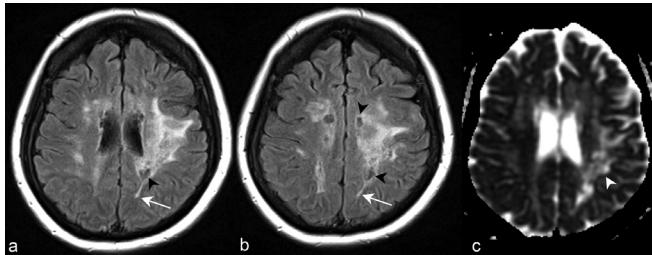


Figure 7. Axial FLAIR images at the level of the corona radiata (a) and centrum semiovale (b) demonstrate a lesion involving much of the left cerebral hemispheric subcortical and deep white matter. Some regions of the lesion demonstrate spindle-like morphology (white arrows). Cystic changes (black arrow heads) within regions of the hemispheric white matter lesion indicate the long-term presence of the abnormality. Apparent coefficient diffusion map of the same patient at the level of the corona radiata (c) demonstrates increased diffusivity of the hemispheric white matter lesion (white arrow head). FLAIR, fluid attenuation inversion recovery.

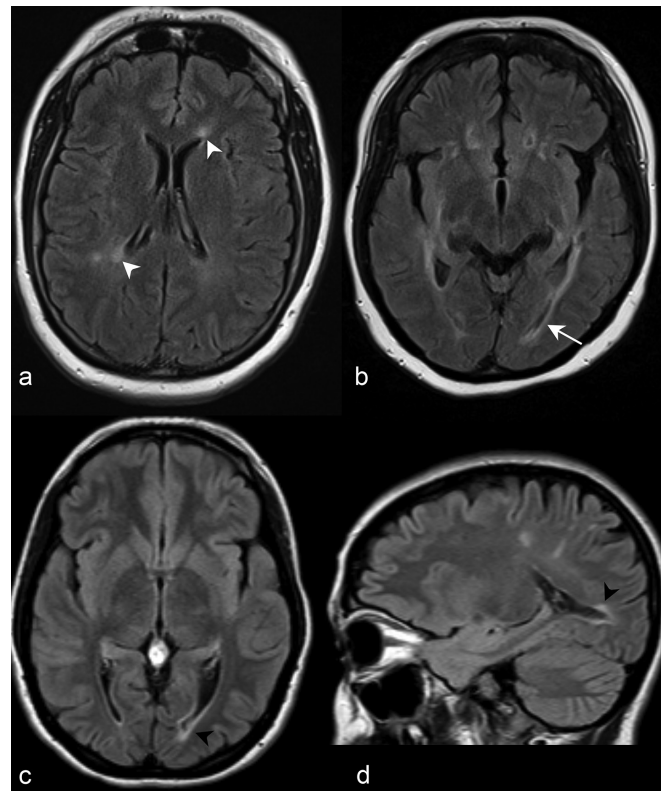


lesions in MS when presenting as an isolated finding. Kim et al observed such lesions in 29% of patients,<sup>8</sup> and such lesions were seen in 4 cases (14%) in our series. Lesions are typically >3 cm in maximal diameter, may be unilateral or bilateral, and involve the subcortical white matter or deep white matter. They are often spindle-like or radial-like in configuration (Figure 7a,b),<sup>8</sup> may exhibit increased diffusivity (Figure 7c) and demonstrate minimal mass effect. Similar to callosal lesions (discussed later), they may decrease in size and result in cystic or cavitory changes with chronicity (Figure 7a,b).<sup>6</sup>

#### Lesions surrounding lateral ventricles

Periependymal lesions surrounding the lateral ventricles (Figure 8) have been reported to be less commonly found than in those in the third and fourth ventricles,<sup>7</sup> with studies observing them in 12 to 40% of patients.<sup>6,8</sup> In contrast, such lesions were seen in 15 of 28 cases (53%) in our series. Both NMOSD and MS may involve the corpus callosum. MS callosal and periventricular lesions are characteristically discrete, ovoid and oriented perpendicularly to the surface of the lateral ventricle (Figure 9a).<sup>4,6</sup> MS callosal lesions also involve the lower margin of the corpus callosum or callosal-septal surface,<sup>9</sup> albeit non-specific and also seen in NMOSD (Figure 10a). In contrast, callosal lesions in NMOSD are broad-based, follow the course of the ependymal lining, are intimately adjacent to the lateral ventricle<sup>8</sup> and often extend nearly the entire longitudinal length of the corpus callosum (Figure 10a).<sup>4,6</sup> Furthermore, a distinct appearance in the acute setting may occur in which large, multifocal, oedematous and heterogeneous callosal lesions may be observed, and has been termed the “marbled pattern” (Figure 10b,c).<sup>9</sup> Full-thickness involvement of the corpus callosum—often termed “arch bridge pattern” (Figures 6a and 10d)—and confluent cerebral white matter extension are also typical (Figures 6a, f and 10e).<sup>8</sup> In the chronic stage, such lesions demonstrate cystic changes (Figure 10e,f), decrease in size, or disappear completely.<sup>9</sup>

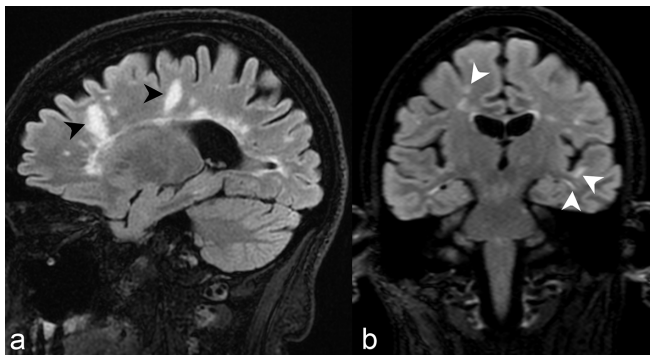
Figure 8. (a) Axial FLAIR imaging at the level of the corona radiata demonstrates increased periependymal signal abnormalities adjacent to the frontal horn and body of the left and right lateral ventricles, respectively (white arrow heads). (b) Axial FLAIR imaging at the level of the hypothalamus in a different patient demonstrates periependymal signal abnormality adjacent to the atrium of both lateral ventricles. Note the posterior extension of the left periependymal lesion to involve the periependymal white matter adjacent to the left occipital horn (white arrow). Axial (c) and sagittal (d) FLAIR of a third patient similarly demonstrate a periependymal lesion adjacent to the left occipital horn of the lateral ventricle (black arrow heads). FLAIR, fluid attenuation inversion recovery.



#### Enhancing lesions

Presence of brain lesion enhancement has been reported in 9 to 36% of patients.<sup>6</sup> The distinctness and specificity of the presence or pattern of brain enhancement in NMOSD is not well described, and enhancement alone is not listed as a NMOSD-typical pattern by the 2015 consensus diagnostic criteria.<sup>4</sup> Nevertheless, when present, subtle, ill-defined cerebral white matter enhancement (“cloud-like”) (Figure 11a) and linear periependymal enhancement adjacent to lateral ventricles (“pencil-thin”) (Figure 11a–c) are most commonly observed. Well-defined nodular (Figure 11b,c), ring (Figure 11d,e), leptomeningeal (Figure 11f) and perivascular enhancement have also been described.<sup>6,10</sup> Although an association between enhancement and acute relapse is well not elucidated, the disappearance of linear periependymal enhancement following an acute relapse has been occasionally reported.<sup>10</sup>

Figure 9. (a) Sagittal 3D FLAIR imaging slightly off midline in a patient diagnosed with MS based on 2010 revised McDonald criteria demonstrates discrete, ovoid callosal lesions perpendicularly oriented to the lateral ventricle surface (Dawson's fingers) and abutting the callosal-septal interface (black arrow heads). Similar to Dawson's fingers, the latter finding has also been described as a characteristic feature of NMOSD, albeit a non-specific one. (b) Coronal 3D FLAIR imaging at the level of the third ventricle of another patient demonstrates multiple juxtacortical white matter lesions typical for MS. The most conspicuous are noted in white arrow heads. 3D, three-dimensional; FLAIR, fluid attenuation inversion recovery; MS, multiple sclerosis.



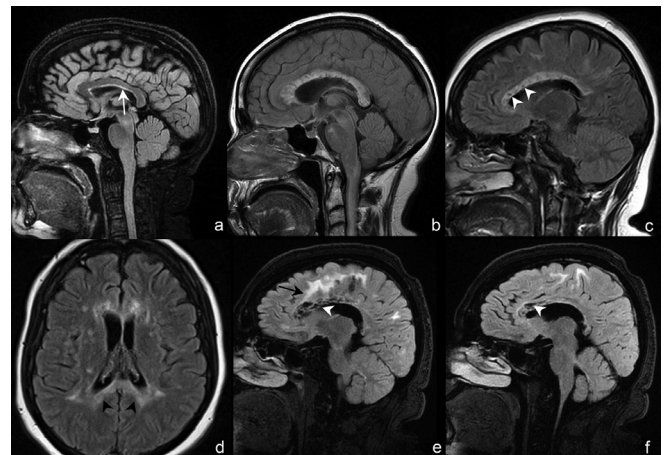
### Diffusivity

The presence and extent of changes on diffusion-weighted imaging are not well described. As mentioned earlier, increased diffusivity on apparent diffusion coefficient maps may be observed in hemispheric white matter lesions (Figure 7c), and is thought to reflect underlying vasogenic oedema associated with acute inflammation.<sup>6,8</sup> Diffusion tensor imaging may reveal changes often occult on conventional MRI, and have demonstrated higher mean diffusivities in regions in both white and grey matter.<sup>11-13</sup> In our series with diffusion-weighted imaging, increased diffusivity was observed in 9 of 28 cases, and may support the hypothesized pathophysiologic mechanism of NMOSD in which there is a breakdown of blood-brain barrier from an autoimmune reaction against AQP4 water channels located on astrocytic foot processes. In contrast, restricted diffusion has also occasionally been observed, and in the context of large or symptomatic callosal lesions during an acute relapse.<sup>14,15</sup>

### CONCLUSIONS

The discovery of the AQP4-Ab, consequent broadening of the NMOSD clinical phenotype, present ability to diagnose NMOSD in the absence of optic nerve or spinal cord involvement, and the growing recognition of brain involvement as one of the hallmarks of NMOSD have altogether allowed imaging to play a more central role in diagnosis. Typical patterns include long CST lesions, hemispheric cerebral white matter lesions and periependymal lesions in the diencephalon, dorsal brainstem, white matter adjacent to lateral ventricles. A strong recognition of the spectrum of MRI brain findings in NMOSD is essential for accurate diagnosis, and particularly in differentiating from

Figure 10. (a) Sagittal 3D FLAIR imaging at midline demonstrates a broad-based callosal lesion intimately associated with the subadjacent lateral ventricle and following the course of the ependymal lining (white arrow). The lesion involves the entire longitudinal length of corpus callosum from rostrum to splenium. (b) Sagittal 2D FLAIR imaging at midline of a different patient demonstrates a swollen corpus callosum with multifocal, heterogeneous and nearly confluent lesions involving the entire short and long axes of the corpus callosum. Such oedematous, heterogeneous appearance may be seen in the acute stage, and has been termed "marbled pattern." (c) Sagittal 2D FLAIR imaging performed 6 months later following the acute stage demonstrates persistent near-confluent signal abnormality, decreased oedema and new volume loss and cystic changes involving the body of the corpus callosum (white arrow heads), which are findings seen in the chronic stage. (d) Axial 2D FLAIR imaging of a different patient at the level of the coronal radiata demonstrates full-thickness involvement of the splenium of the corpus callosum (black arrow heads), a finding termed "arch bridge pattern," given the posteriorly concave appearance. Sagittal 3D FLAIR images of another patient slightly off (e) and at midline (f) demonstrate extensive cystic changes of the genu and body of the corpus callosum (white arrow heads). Frontal deep white matter lesions extend from the corpus callosum superficially to the subcortical white matter (e, black arrow). 2D, two-dimensional; 3D, three-dimensional; FLAIR, fluid attenuation inversion recovery.



MS. Future studies investigating associations between imaging findings and remission may allow imaging to play a more central role in assessment of treatment response.

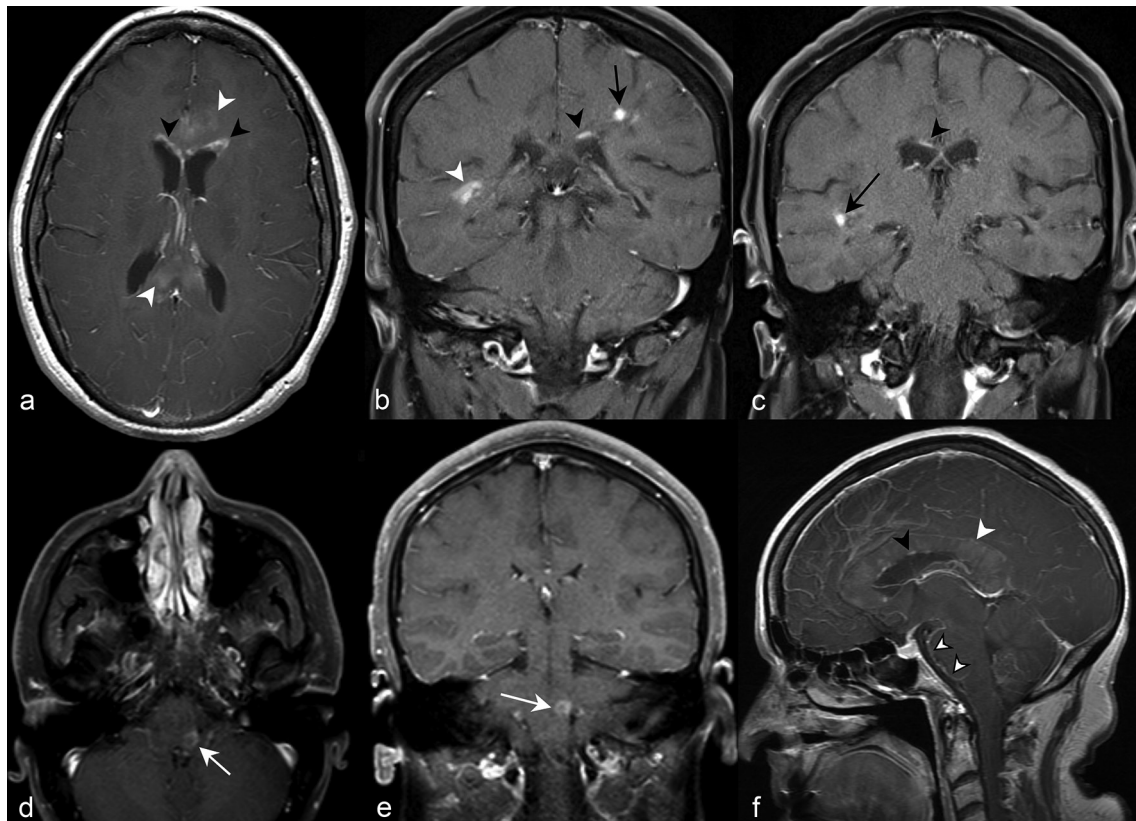
### ACKNOWLEDGEMENTS

The authors are thankful to George Hutton, MD. and Rola Mahmoud, MD. and for assisting in the review and procurement of the NMOSD cases.

### ETHICAL APPROVAL

Approval for the study was obtained from the Baylor College of Medicine Institutional Review Board. Informed consent was exempted.

Figure 11. (a) Axial post-contrast  $T_1$  weighted imaging at the level of the thalami demonstrates subtle “cloud-like” enhancement of the genu and splenium of the corpus callosum (white arrow heads). There is periependymal enhancement predominantly in a linear to curvilinear configuration anteriorly adjacent to both frontal horns (black arrow heads). (b) Coronal post-contrast  $T_1$  weighted imaging in a different patient further depicts the linear periependymal “pencil-thin” enhancement suprajacent to the left lateral ventricle (black arrow head). Well-defined nodular (black arrow) and more confluent enhancement (white arrow head) in the parietal and temporal white matter, respectively, are also depicted. (c) More anteriorly, coronal imaging demonstrates more regions of “pencil-thin” (black arrow head) and nodular enhancement (black arrow). Axial (d) and coronal (e) post-contrast  $T_1$  weighted images in a different patient demonstrate ring enhancement of the left dorsal medulla in the region of the area postrema (white arrows). (f) Sagittal post-contrast  $T_1$  weighted imaging at midline demonstrates leptomeningeal enhancement along the interpeduncular and prepontine cisterns (outlined white arrow head). Numerous discontinuous foci of “pencil-thin” enhancement (black arrow head) and “cloud-like” enhancement (white arrow head) involve the corpus callosum.



## REFERENCES

1. Wingerchuk DM, Lennon VA, Lucchinetti CF, Pittock SJ, Weinshenker BG. The spectrum of neuromyelitis optica. *Lancet Neurol* 2007; **6**: 805–15. doi: [https://doi.org/10.1016/S1474-4422\(07\)70216-8](https://doi.org/10.1016/S1474-4422(07)70216-8)
2. Pittock SJ, Lennon VA, Krecke K, Wingerchuk DM, Lucchinetti CF, Weinshenker BG. Brain abnormalities in neuromyelitis optica. *Arch Neurol* 2006; **63**: 390–6. doi: <https://doi.org/10.1001/archneur.63.3.390>
3. Wingerchuk DM, Lennon VA, Pittock SJ, Lucchinetti CF, Weinshenker BG. Revised diagnostic criteria for neuromyelitis optica. *Neurology* 2006; **66**: 1485–9. doi: <https://doi.org/10.1212/01.wnl.0000216139.44259.74>
4. Wingerchuk DM, Banwell B, Bennett JL, Cabre P, Carroll W, Chitnis T, et al. International consensus diagnostic criteria for neuromyelitis optica spectrum disorders. *Neurology* 2015; **85**: 177–89. doi: <https://doi.org/10.1212/WNL.0000000000001729>
5. Min JH, Kim BJ, Lee KH. Development of extensive brain lesions following fingolimod (FTY720) treatment in a patient with neuromyelitis optica spectrum disorder. *Mult Scler* 2012; **18**: 113–5. doi: <https://doi.org/10.1177/1352458511431973>
6. Kim HJ, Paul F, Lana-Peixoto MA, Tenembaum S, Asgari N, Palace J, et al. MRI characteristics of neuromyelitis optica spectrum disorder: an international update. *Neurology* 2015; **84**: 1165–73. doi: <https://doi.org/10.1212/WNL.0000000000001367>
7. Pittock SJ, Weinshenker BG, Lucchinetti CF, Wingerchuk DM, Corboy JR, Lennon VA. Neuromyelitis optica brain lesions localized at sites of high aquaporin 4 expression. *Arch Neurol* 2006; **63**: 964–8. doi: <https://doi.org/10.1001/archneur.63.7.964>
8. Kim W, Park MS, Lee SH, Kim SH, Jung IJ, Takahashi T, et al. Characteristic brain magnetic resonance imaging abnormalities in central nervous system aquaporin-4 autoimmunity. *Mult Scler* 2010; **16**: 1229–36. doi: <https://doi.org/10.1177/1352458510376640>
9. Nakamura M, Misu T, Fujihara K, Miyazawa I, Nakashima I, Takahashi T, et al. Occurrence of acute large and edematous callosal lesions in neuromyelitis optica. *Mult Scler* 2009; **15**:

- 695–700. doi: <https://doi.org/10.1177/1352458509103301>
10. Pekcevik Y, Orman G, Lee IH, Mealy MA, Levy M, Izbudak I. What do we know about brain contrast enhancement patterns in neuromyelitis optica? *Clin Imaging* 2016; **40**: 573–80. doi: <https://doi.org/10.1016/j.clinimag.2015.07.027>
11. Rocca MA, Agosta F, Mezzapesa DM, Martinelli V, Salvi F, Ghezzi A, et al. Magnetization transfer and diffusion tensor MRI show gray matter damage in neuromyelitis optica. *Neurology* 2004; **62**: 476–8. doi: <https://doi.org/10.1212/01.WNL.0000106946.08741.41>
12. Yu C, Lin F, Li K, Jiang T, Qin W, Sun H, et al. Pathogenesis of normal-appearing white matter damage in neuromyelitis optica: diffusion-tensor MR imaging. *Radiology* 2008; **246**: 222–8. doi: <https://doi.org/10.1148/radiol.2461062075>
13. Yu CS, Lin FC, Li KC, Jiang TZ, Zhu CZ, Qin W, et al. Diffusion tensor imaging in the assessment of normal-appearing brain tissue damage in relapsing neuromyelitis optica. *AJNR Am J Neuroradiol* 2006; **27**: 1009–15.
14. Jacob A, McKeon A, Nakashima I, Sato DK, Elson L, Fujihara K, et al. Current concept of neuromyelitis optica (NMO) and NMO spectrum disorders. *J Neurol Neurosurg Psychiatry* 2013; **84**: 922–30. doi: <https://doi.org/10.1136/jnnp-2012-302310>
15. Sato D, Fujihara K. Atypical presentations of neuromyelitis optica. *Arq Neuropsiquiatr* 2011; **69**: 824–8. doi: <https://doi.org/10.1590/S0004-282X2011000600019>